UCRL-JC-118383
PREPRINT

High-Speed, High-Resolution Observations of Shaped-Charge Jets Undergoing Particulation

K. Winer
D. Breithaupt
L. Shaw
S. Muelder
D. Baum

This paper was prepared for submittal to the
15th International Symposium on Ballistics
Jerusalem, Israel
May 21-24, 1995

February 28, 1995

Lawrence Livermore National Laboratory

15th International Symposium on Ballistics
Jerusalem, Israel, 21 - 24 May, 1995

HIGH-SPEED, HIGH-RESOLUTION OBSERVATIONS OF SHAPED-CHARGE JETS UNDERGOING PARTICULATION

K. Winer, D. Breithaupt, L. Shaw, S. Muelder, and D. Baum

Lawrence Livermore National Laboratory, P.O. Box 808 L-35, Livermore, California 94551

Image-converter (IC) camera photography has provided spectacular images and quantitative records of liner collapse and early jet formation in shaped charges. We have extended the application of the IC camera to observations of shaped-charge jet surfaces undergoing particulation. Sequential, high-resolution photographs were taken following the same 10-cm portion of jet at 2.5-µs intervals. Simultaneous color rotating-mirror framing camera photographs and 450-keV flash x-ray radiographs were also taken of the same region. This combination provides a detailed record of the evolution of surface structure during jet necking and particulation. In the high-resolution photographs, individual features on the jet surfaces as small as ~100 µm can easily be detected and followed as they evolve over time. The jet surface structure is rough with overlapping slip dislocation lines running along the surface at 45° to either side of the jet axis. This is similar to the texture that develops in long rods undergoing static tension. We discuss the implications of these images for increasing jet particulation times.

INTRODUCTION

We have demonstrated that high-resolution image-converter (IC) camera photography can provide spectacular images of shaped-charge jets [1,2]. The combination of large 75-mm-diameter image plane, short 20-ns exposure times, and pulsed-laser illumination provides clear, sharp images of liner and jet surfaces unobscured by luminous air shocks or motion blur. We have applied this capability to produce detailed, quantitative records of the liner collapse and early jet formation processes in conical Cu-lined shaped charges [3,4]. In these experiments, the jet surface morphology was observed to be smooth and uniform during initial jet formation. When the jet tip reached one or two charge diameters, the jet surface took on a speckled texture. We observed this behavior in all experiments carried out with Cu jets where the jet surface could be clearly seen. This texture persisted and grew in size as the jets stretched to 6.4 charge diameters. This initial surface texture could represent the perturbations from which jet necking and eventual particulation proceed. Examples of this texturing are shown in Fig. 1.

The time over which conical Cu-lined shaped-charge jet surfaces can be clearly seen extends beyond that at which jet particulation occurs. We have imaged Viper shaped-charge jet surfaces at various stages of particulation and have observed complex surface structure coupled with areas of strong laser-light reflection. These areas might be characterized by different material and/or thermal properties, or might correspond to internal portions of the jet exposed by severe surface fracturing. In order to further investigate jet particulation in general and this enhanced reflection phenomenon in particular, we have extended the application of the IC camera to detailed observations of Viper shaped-charge-jet surfaces undergoing particulation.

Sequential, high-resolution photographs were taken following the same 10-cm portion of jet at 2.5-µs intervals. Simultaneous color Cordin Model 121 rotating-mirror framing camera photographs and 450-keV flash x-ray radiographs were also taken of the same region. This combination provides a detailed record of the evolution of surface structure and texture during jet necking and particulation.

Figure 1 IC camera photographs of a Viper jet showing the onset and evolution of surface texture. The black lines show where the texture is made visible by specular reflection of the laser light.

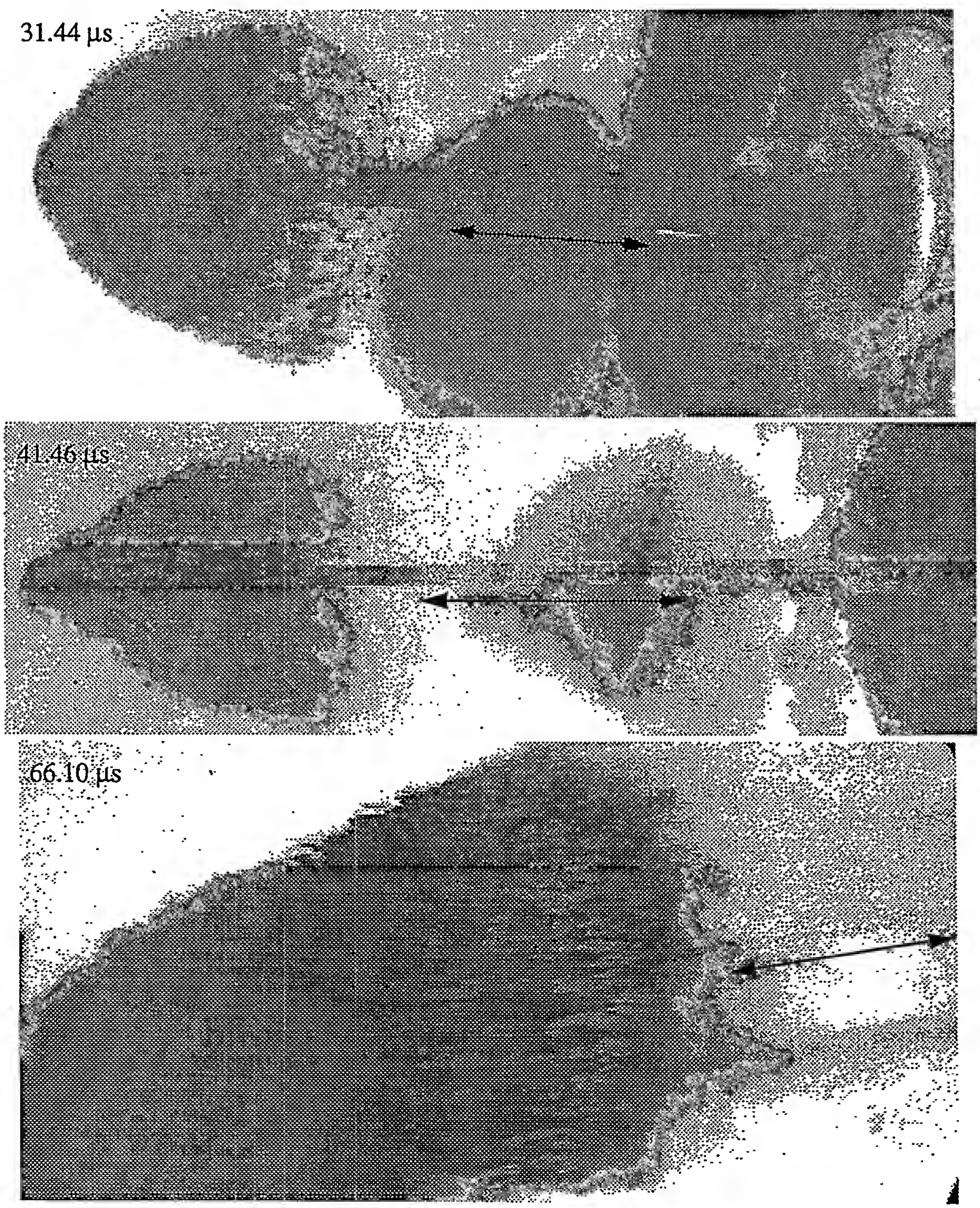

DESCRIPTION OF THE EXPERIMENTS

The Viper shaped charge employs a 77 g, 44° conical copper liner 1.2-mm thick at the hemispherical apex and 1.0-mm thick elsewhere. The high explosive charge consists of 427 g of LX-14 pressed over the liner, after which it is lightly machined at room temperature to a final 65-mm diameter. A modified aluminum case was designed to accomodate the LLNL-designed precision-initiation-coupler with LX-10 booster and electronic bridge-wire detonator assembly. The time from bridge-wire burst to main-charge breakout was measured to be 5.82 μs. All times quoted here are from bridge-wire burst.

The shaped-charge performance was simulated using the two-dimensional LLNL C-language-based Arbitrary-Lagrangian-Eulerian hydrocode Cale [5]. The simulation predicted stable jet development with a tip speed of 9.28 mm/μs for the Viper jet. The jet mass and velocity distributions calculated for the Viper agree well with experimental results [3]. The simulated performance characteristics were used as the basis for the design of the experiments.

The main experimental diagnostics consisted of optical records taken with two LLNL-designed Cordin model 121 rotating-mirror framing cameras and eight LLNL-developed image-converter (IC) cameras. 450-keV x-ray radiography was also used to characterize the shaped-charge jets. The framing camera images were recorded on Kodak Ektachrome film with ~200-ns frame exposure times. The records from the framing camera consisted of 25 frames separated by 1.1 μs intervals for a total record of ~28 μs. High-explosive-driven argon candles were used to provide front-lit, broad-band illumination for color framing camera photography. The IC camera images were recorded on Kodak T-Max 3200 monochrome film with 20-ns exposure times. A Q-switched ruby laser system provided eight individual light pulses that were synchronized with the IC camera frames and passed through a ground-glass diffuser positioned near the experiment to provide illumination. A camera-mounted 1.5-nm band-pass filter centered at the 694.3-nm ruby laser wavelength was used to exclude extraneous light.

We carried out three experiments with the Viper shaped charge in order to observe the jet surface during jet necking and breakup. In the first experiment (1410-B3), two frames of the IC camera were focused on a 15-cm portion of the jet (51 to 66 cm from the charge face) that spanned the velocity range 0.51-0.65 cm/μs and were photographed at 123 μs and 127 μs. One frame was focused on a 30-cm portion of the jet (45 to 75 cm from the charge face) that spanned the velocity range 0.41-0.67 cm/μs and was photographed at 135 μs. In the second experiment (1410-B9), the IC camera was focused on a 15-cm portion of the Viper jet that spanned the velocity range 0.68-0.86 cm/μs. Eight sequential frames between 108.0 μs and 125.5 μs with a 2.5 μs interval were photographed corresponding to the area between 60 and 90 cm from the charge base. In the third experiment (1410-B10), the IC camera was focused on a 10-cm portion of the Viper jet that spanned the velocity range 0.53-0.67 cm/μs. Eight sequential frames between 115.0 μs and 132.5 μs with a 2.5 μs interval were photographed corresponding to the area between 50 and 70 cm from the charge base.

In all experiments, the frames were chosen to capture the jet both before and after the particulation time for that portion of the jet as determined in previous experiments from x-ray radiography. Rotating-mirror framing camera photography was carried out on 30-cm portions of the jet that included the spatial range of the IC camera photographs. 450-keV x-ray radiography of a 70-cm wide area containing the optical region of interest was also obtained.

EXPERIMENTAL RESULTS

Traditional shaped-charge jet experimental diagnostics consist of flash x-ray radiography and, if available, rotating-mirror framing camera photography. These diagnostics are valuable for measuring jet coherence, jet tip time of arrival, particulation times, and the shaped-charge virtual origin. However, they provide few details regarding the nature and metallurgical state of the jet surface as can be seen in the images of Viper jets shown in Fig. 2.

Figure 2 Rotating-mirror framing camera image (left) and 450-keV flash x-ray radiographs (right) of a Viper jet.

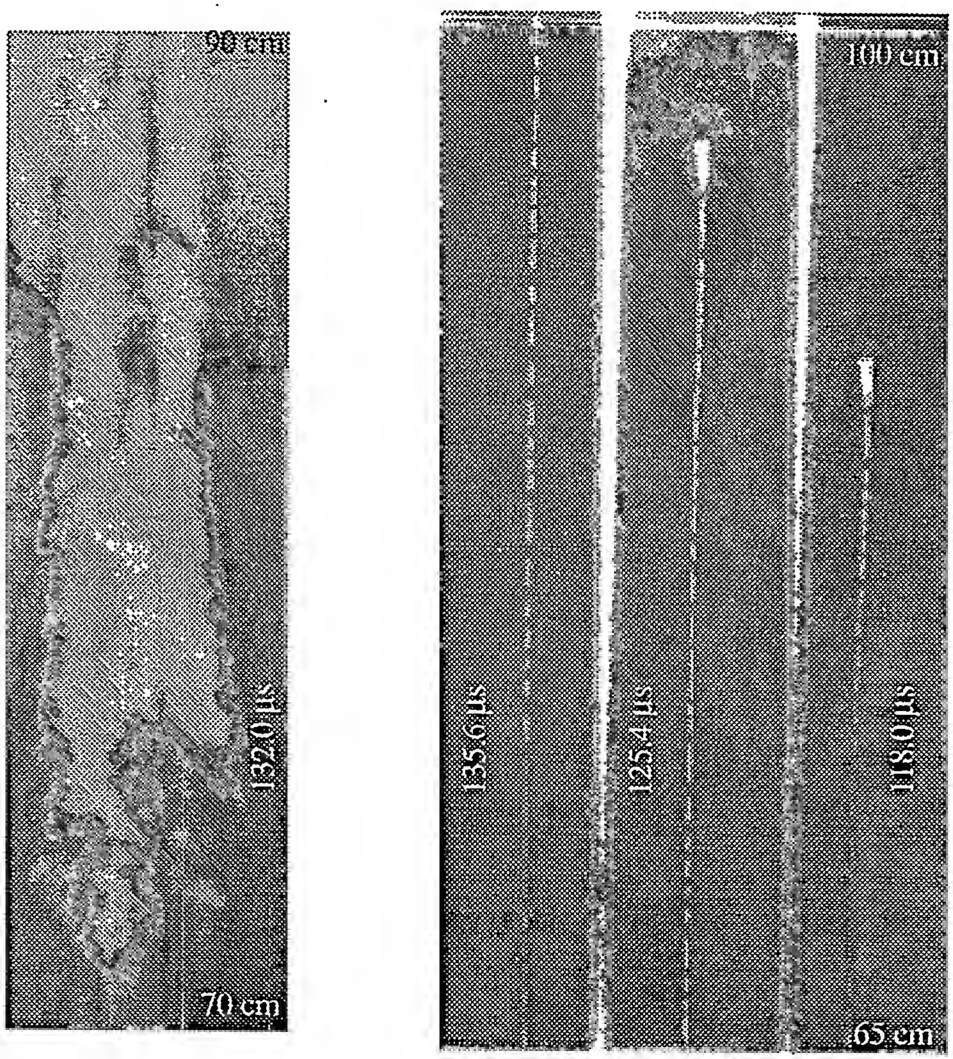

The rotating-mirror framing camera image of the Viper jet is mostly obscured by the low-density Cu debris from the jet tip and the air-ionization light from the shock front surrounding the jet near its tip. The portion of the jet far enough away from these effects to be seen in the image suffers from motion blur due to the ~200-ns exposure time.

The 450-keV flash x-ray radiography shows the individual particles of the Viper jet well separated from each other over most of the field of view. Although further details in the shadowgraphy might become apparent if the energy were reduced and the magnification were

increased (*i.e.*, the field of view decreased), it is unlikely that these could amount to much more than an improvement in the relative density contrast.

The high spatial and temporal resolution of the image-converter camera are ideally suited to imaging shaped-charge jet surfaces. The pulsed-laser illumination eliminates obscuring extraneous light and motion blur. Together with the complementary optical and radiographic diagnostics, the IC camera images provide a detailed record of jet surface evolution during jet necking and particulation as shown below.

In the first experiment, the field of view is sufficiently far from the jet tip (at ~100 cm) that little obscuration was encountered. The results of the IC camera photography are compiled in Fig. 3. Individual particles can readily be seen. Most of the particles are quite similar in size and general shape. A hint of surface structure can be seen at places along the jet. Particularly striking are the bright laser-light reflections that seem to be correlated with the necking regions between the particles. The jet receives a uniform, diffuse laser-light illumination. The bright spots along the jet, therefore, must be regions that have acquired a large reflectivity relative to the remainder of the jet.

This behavior might be due to the fact that the surface at various points along the jet is oriented such as to return a large portion of the laser light toward the camera. This geometric effect is also observed in Fig. 1, where the surface texture is made apparent by variations in brightness that do not appear as strongly in IC camera images of Viper jets at similar times but viewed at different angles. These bright spots and brightness variations might also be due to underlying changes in the material properties of the jet surface. For example, the correlation between the bright spots and the jet necking regions might be due to the exposure of internal portions of the jet whose temperature is expected to be significantly higher than that at the surface.

One way to understand this behavior better is to extend the experiment to follow the same region of jet over a longer time frame. This was the intent of the next two experiments.

Figure 3 IC camera images of the particulating Viper jet at the indicated times.

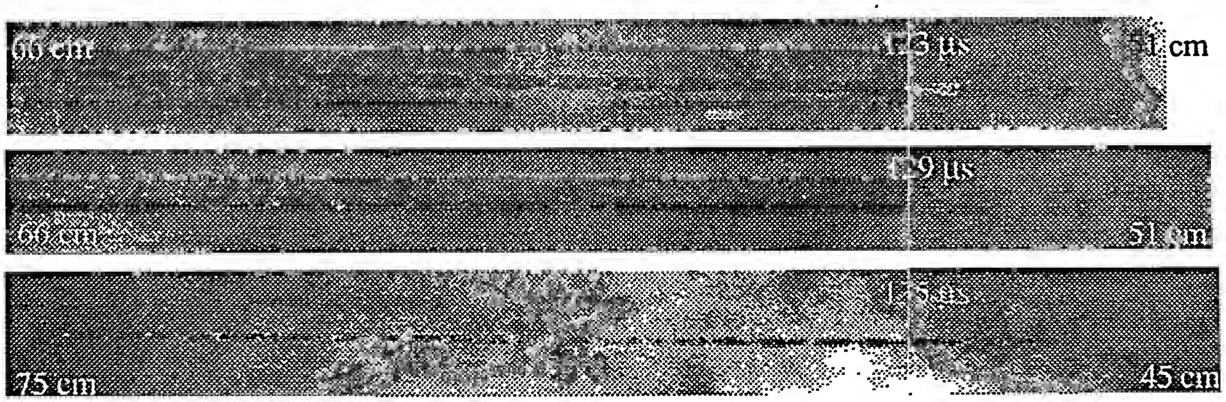

In the second experiment, we attempted to image a different portion of the surface closer to the jet tip. Low-density copper debris from the jet tip obscured the jet surface sufficiently that little detail except the presence of individual particles in the later frames can be discerned.

In the third experiment, the field of view was taken to be similar to that from the previously

Figure 4 IC camera images of the particulating Viper jet at the indicated times.

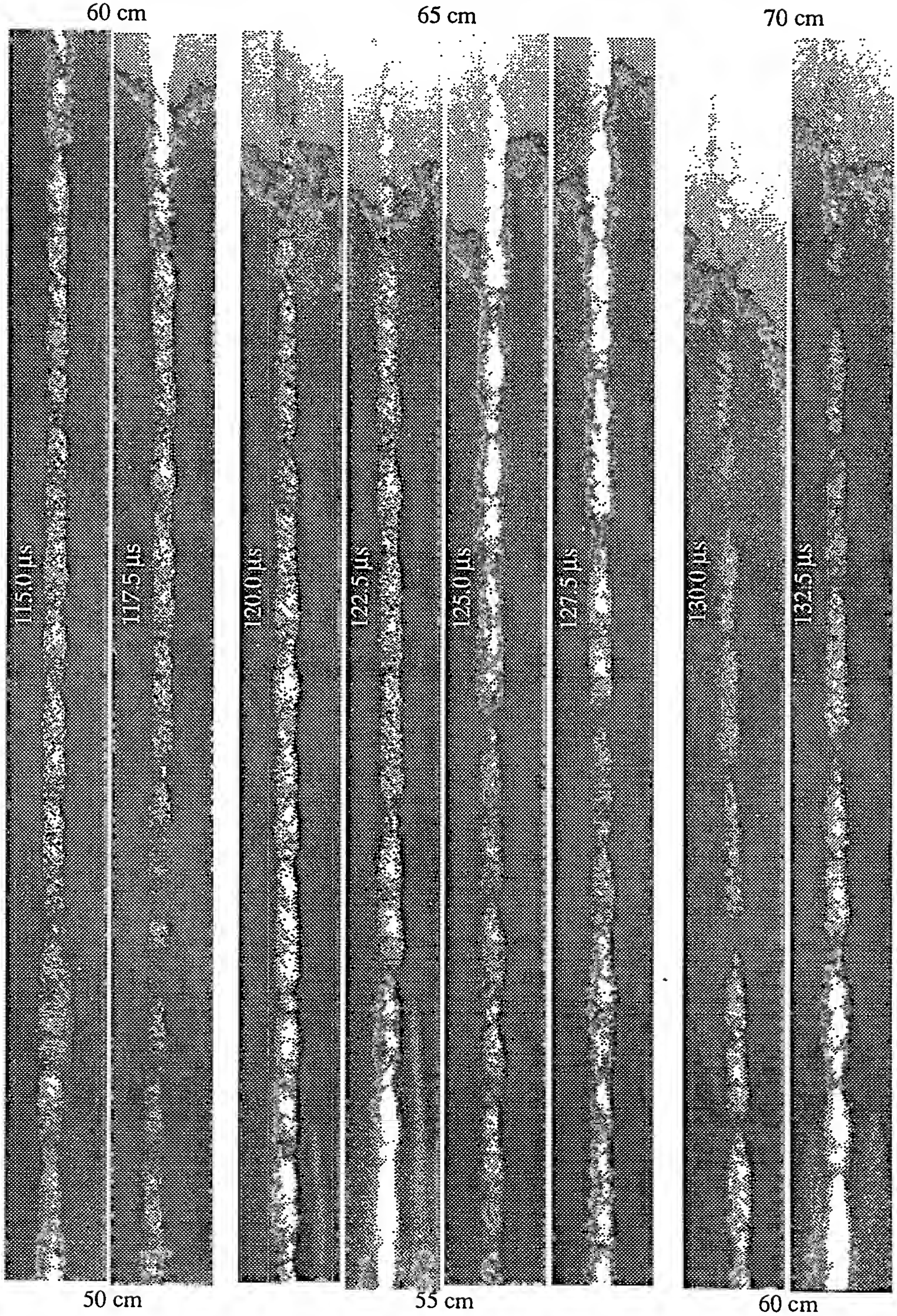

successful first experiment and the magnification was increased. The results of the IC camera photography are compiled in Fig. 4. Again, individual particles can be clearly seen. The particles are between 4 and 5 mm in length and are connected by jet material in varying stages of necking. The detail that can be observed on the jet surface is remarkable; features as small as 100 microns can clearly be seen in the images. The surface is rough and characterized by complex patterns. The jet surface displays slip dislocation lines running at 45° with respect to the jet axis. These are similar to the dislocation lines observed in solid metal rods undergoing static tension. It seems clear from this observation that the Viper jet surface is solid and is not melted.

In the sequence of images in Fig. 4, the evolution of the jet over the 17.5 μs time frame can be observed. As in Fig. 3, individual particles have begun to form which are separated by necking regions. The separation between particles can be seen to increase with time as the jet stretches. Approximately 2.5 cm less of the jet appears in the latest frame than appears in the earliest one due to stretching. Eventually, in the latest image, the particles near the top of the field of view appear to have separated from each other. The jet surface structure also evolves with time, but the variation in photodetector quality among the various IC cameras obscures the finer detail in some of the images.

In the x-ray radiographs of Fig. 2, the jet appears to be fully particulated at the time the IC camera pictures were taken. It is interesting that in the high-resolution IC camera images the jet particles, with one exception, have yet to completely separate. Although only a small overlap exists between the portion of the jet that appears in the x-ray radiographs and the portion of jet that appears in the IC camera images, it appears that the necking regions between the particles might be lower in density as well as mass compared to the main particles. This means that measurement of particulation times that rely on x-ray radiography are only valid in a relative sense. The relative density of the low-mass material connecting the particles measured by the radiography probably varies depending on the x-ray energy, flux, and magnification resulting in different particulation time estimates.

IMPLICATIONS FOR PARTICULATION TIMES

While the images of jet surfaces caught in the act of particulating are spectacular in their detail and novelty, they do not provide *by themselves* any deeper understanding into the process of jet breakup. The surface details visible in Fig. 4, however, do suggest further experiments that might increase our understanding of particulation.

Copper, like most metals, responds to deformation by forming lattice defects such as dislocations. The dislocations pile up at grain boundaries and areas of high impurity concentration and impede further material flow. The highly reflective nature of the necking regions between jet particles seen in Fig. 3 might indicate that jet necking occurs where lattice defect concentrations are small, and the surface is smooth, relative to the rest of the jet. There seems to be some regularity in the necking process as indicated by the nearly constant particle shapes and sizes. This suggests that jet particulation might be described by some simple physics. Images such as those shown in Figs. 3 and 4 made with jets of varying impurity concentrations and/or processing histories could help to understand the effects of jet microstructure on particulation.

The fact that features similar to slip dislocation lines appear on the jet surface during stretching and particulation suggests the possibility that simple static tension tests might provide a useful

vehicle for exploring the relationship between necking, which is an essential step in jet particulation, and jet material properties and geometry. The average strain rate in the Viper jet near the particulation time is approximately $1 \times 10^4 s^{-1}$. This is within the range accessible by Hopkinson-type tensile experiments that could be performed on Cu rods of geometries similar to a Viper jet in order to provide additional understanding of the IC camera results presented here.

ACKNOWLEDGMENTS

We thank Denise Kuklo for superior engineering support, and Jack Lowry and the crew at Bunker 851 where the experiments were carried out. Work performed under the auspices of the U.S. Department of Energy by Lawrence Livermore National Laboratory under contract #W-7405-Eng-48. This work was supported in part by the Joint DOD/DOE Munitions Technology Development Program.

REFERENCES

[1] L.L. Shaw, S.A. Muelder, A.T. Rivera, J.L. Dunmire, and R.D. Breithaupt, "Electro-Optic Frame Photography with Pulsed Ruby Illumination," *20th International Congress on High Speed Photography and Photonics*, Victoria, B.C., September 21-25, 1992.

[2] D.W. Baum, L.L. Shaw, and C.A. Honodel, "Application of High-Resolution Optical Technique to Shaped-Charge Jet Formation," *13th International Symposium on Ballistics*, Stockholm, May 1992.

[3] D. Baum, L. Shaw, S.C. Simonson, and K. Winer, "Liner Collapse and Early Jet Formation in a Shaped Charge," *Proc. 14th Int'l Ballistics Symposium*, Quebec City, Canada, Sept. 26-29 1993.

[4] K. Winer, L. Shaw, S. Muelder, D. Breithaupt, and D. Baum, "Dynamic Behavior of a Shear-Formed Shaped-Charge Liner," *Propellants, Explosives, and Pyrotechnics* **18** (1993) 345-351.

[5] R. Tipton, private communication.